

Experimental and Numerical Investigation to Evaluate the Performance of U-Longitudinal Finned Tube Heat Exchanger

Prof. Dr. Qasim Saleh Mahdi

Mechanical Engineering Dept., College of Engineering , Al-Mustansiriyah University

Lecturer. Dr. Sahar Abdul Fattah

Mechanical Engineering Dept., College of Engineering , Al-Mustansiriyah University

Firas Abd ali Abbas

Mechanical Engineering Dept., College of Engineering , Al-Mustansiriyah University

Abstract:

Experimental and numerical investigation has been performed in this work to evaluate the performance for U-longitudinal finned tube heat exchanger. Four pairs of U-shaped longitudinal fins were selected and manufactured from copper material and welded on the straight copper tube. The inner tube is inserted inside insulated galvanized tube, sheet and roll insulation (arm flux) and glass wool have been utilized to cover inner and outer surface of galvanized tube for reducing heat losses. Air at various mass flow rates (0.03 to 0.07)kg/sec flows through annuli and de-ionized water at Reynold's numbers ranging from (270 to 1900) flows through the inner tube. Performance of (smooth and finned) tube heat exchanger was investigated experimentally. Experimental results showed (1.744 to 2.534) enhancement ratio when using U-longitudinal fins. Empirical correlations for air, water were represented by Nusselt's number. Numerical simulation has been carried out on present heat exchanger to analyze flow field and heat transfer using FLUENT package 14. The comparison between experimental work and numerical results showed good agreement.

Keywords: heat exchanger, finned tube, ANSYS FLUENT.

تحقيق عملي ونظري لتقييم أداء مبادل حراري من نوع الأنبوب المزعنف بزعانف طولية على شكل حرف U

فراس عبد علي
قسم الهندسة الميكانيكية
الجامعة المستنصرية

م.د. بسحر عبد الفتاح عبود
قسم الهندسة الميكانيكية
الجامعة المستنصرية

إ.د. قاسم صالح مهدي
قسم الهندسة الميكانيكية
الجامعة المستنصرية

الخلاصة

في هذه الدراسة، تم انجاز تحقيق عملي وعددي لمبادل حراري من نوع الانبوب المزعنف بزعانف طولية على شكل حرف (U) من اجل دراسة ادائه الحراري. اربعة ازواج من الزعانف الطولية ذات شكل (U) تم تصميمها وتصنيعها من مادة النحاس وثبتت على انبوب نحاس الذي اولج داخل انبوب مصنع من مادة الكلفنايز ومغزول بعوازل من الداخل والخارج لتقليل الحرارة المفقودة. هواء عند معدلات تدفق كتلية تتراوح بين (0.03 الى 0.07) كغم/ثانية يجري خلال الفراغ الحلقى وماء منزوع الايونات ذو ارقام رينولدز تتراوح بين (270 الى 1900) يجري خلال الانبوب الداخلي. اداء المبادل الحراري بالحالتين (الاملس والمزعنف) تمت دراسته. النتائج العملية بينت ان نسبة التحسين كانت (1.744 الى 2.534) في حال استخدام المبادل الحراري ذو الانبوب المزعنف. علاقات تجريبية لجانب الهواء والماء تم تقديمها بدلالة رقم نيسلت. محاكاة عددية تم انجازها للمبادل الحراري لتحليل جريان المانع وانتقال الحرارة باستخدام البرنامج المتخصص *ANSYS FLUENT14*. بينت المقارنة بين النتائج العملية والعديدية وجود تطابق مقبول.

List of symbols

English symbols

Symbol	Description	Units
A_c	Cross section area of annuli	m^2
A, A_s	Surface area	m^2
C_p	Specific heat	$J/kg. ^\circ C$
$C_{1\epsilon}, C_{2\epsilon}, \sigma_\epsilon, \sigma_\chi$	Model constants	...
D	Diameter of insulated pipe	m
D_e	Equivalent diameter of annuli	m
D_{hu}	Hydraulic diameter of annuli	m
d	Diameter of inner tube	m
h	Heat transfer coefficient	$W/m^2. ^\circ C$
H	Height	m
k	Thermal conductivity	$W/m. ^\circ C$
l	Length	m
\dot{m}	Mass flow rate	kg/sec
N_f	Number of fins	...
Nu	Nusselt's number	...
pr	Prandtl's number	...
P	Perimeter	m
P	Pressure	Pa
Q	Heat dissipation	W
Re	Reynold's number	...
T	Temperature	$^\circ C$

T_{ci}	Inlet temperature of cold fluid	°C
T_{co}	Outlet temperature of cold fluid	°C
T_{hi}	Inlet temperature of hot fluid	°C
T_{ho}	Outlet temperature of hot fluid	°C
U	Overall heat transfer coefficient	$W/m^2 \cdot ^\circ C$
V	Velocity	m/sec
(u, v, w)	Velocity component	m/sec
$(\bar{u}, \bar{v}, \bar{w})$	Mean velocity component	m/sec
(u', v', w')	Fluctuating velocity component	m/sec
Z/d	Axial distance ratio	...

Greek symbols

Symbol	Description	Unit
ϵ	Heat exchanger effectiveness = $\frac{Q_h}{(\dot{m}Cp)_{min}(T_{hi}-T_{ci})}$...
δ	Fin thickness	m
μ	Dynamic viscosity	$kg/m \cdot sec$
ν	Kinematic viscosity	m^2/sec^2
μ_t	Turbulence viscosity	$kg/m \cdot sec$
ρ	Density	kg/m^3
α	Thermal diffusivity	m^2/sec
ξ	Efficiency	...
\mathcal{K}	Turbulent kinetic energy generation	m^2/sec^2
ϵ	Turbulent kinetic energy dissipation	m^2/sec^3

Subscripts

Symbol	Description
c	Cold
f	Fin
h	Hot
i	Inner
m	Mean
max	Maximum
min	Minimum
o	Outlet
s	Surface
t	Total
u	Unfinned
w	Wetted

Abbreviations

Symbol	Description
LMTD	Logarithmic mean temperature difference
NTU	Number of transfer units = $\frac{UA}{(\dot{m}Cp)_{min}}$

1. Introduction

Energy and materials saving considerations as well as economic incentives have led to an effort to produce more efficient heat exchange equipment's. Common thermal hydraulic goals are to reduce the size of a heat exchanger required for a specified heat duty, to upgrade the capacity of an existing heat exchangers and to reduce the approach temperature difference for the process streams or to reduce the pumping power.

Enhancement techniques can be classified either as passive or active techniques. Passive techniques which require no direct application of external power and the additional power needed to enhance the heat transfer is taken from the available power in the system. They generally use surface or geometrical modifications to the flow channel such as extended surfaces, treated surfaces. Active techniques which require external power such as mechanical aids, surface vibration^[1]. Longitudinal fins have proven to be most efficient kinds of fins in many applications. They are generally used in condensing applications and for various fluids in double pipe and multi-tube heat exchanges, fired heaters, gas coolers and tank heaters. Therefore, many researchers are focused on this kind of heat exchanger. **Taborek**^[2] updated sketchy methods for double pipe heat exchangers especially for longitudinal finned tubes. Areas and conditions for the most useful applications were outlined. Calculation methods are presented for plain double pipe units, as well as finned tube units, with a new development in the important transition region with cut and twisted turbulence promoters. Equations for the mean temperature difference for units with flow in series-parallel were given. **Fabbri**^[3] studied the heat transfer enhancement of optimized dissipates with longitudinal fins of a symmetrical cross section and compared it with asymmetrical fins. A finite element model was proposed to obtain velocity and temperature distributions by genetic algorithm to determine the highest value of heat transfer coefficient under different conditions. **Yu and Tao**^[4] performed study to measure pressure drop and heat transfer characteristics of annular tubes with wave-like longitudinal fins at uniform axial heat input using air as the working fluid on both the entrance and fully developed regions. Five experiments in the annular tubes with waves equal to 4,8,12,16 and 20 at turbulent flow. It was found that under the three constraints all the wave-like finned tubes can enhance heat transfer and the best wave number was 20. **Mir et al.**^[5] carried out numerical simulation of finned annulus in steady, laminar convection heat transfer in the fully developed at the constant heat input. Boundary fitted curvilinear coordinates were used. Various heat transfer and fluid flow were investigated. The results showed a good comparison with the literature results. **Syed et al.**^[6] performed numerical simulation of finned annulus in the steady and laminar convection in the thermal entry region, fully developed flow at uniform heat flux. Finite difference based marching procedure was used. The results indicated that the Nusselt's number has complex depending on the geometric variables. The validation of the simulation

was performed by comparison with open literature. **Iqbal** et al.^[7] investigated of the optimal longitudinal fins on the outer surface of the inner pipe enclosed within a concentric outer pipe in laminar and fully developed flow at uniform heat flux. The fin–shape was triangular as the initial profile. The results showed that the optimum fin–shape is dependent on the number of fins, the ration of radii, the number of control points and characteristic length. The enhancement in Nusselt's number was up to 138%, 312% and 263% for trapezoidal, triangular and parabolic shapes for equivalent diameter while 212%, 59% and 90% respectively for hydraulic diameter. It seems from open literature, there are some researches of longitudinal finned tube heat exchangers. These types of fins need additional researches especially when using (U) shaped fins. Therefore, present work focused on experimental and numerical study of thermal performance of U-longitudinal finned tube heat exchanger.

2. Theoretical Analysis

Present study consists two fluid flow inside heat exchanger in counter flow arrangement as shown in **Figure (1)**. cold air is forced to flow through annuli and hot de-ionized water is passes through inner tube. Steady state condition, insulated outer surface of heat exchange and no phase changer have been assumed during the analysis of present heat exchanger. Under these conditions the heat dissipation of both sides^{[8] [9]}:

$$Q_c = \dot{m}_c c p_c (T_{co} - T_{ci}) \text{ and } Q_h = \dot{m}_h c p_h (T_{hi} - T_{ho}) \quad \dots(1)$$

The heat dissipation during this study is calculated by using the temperature difference on the water side in equation (1)^[10]

Heat transfer coefficient of hot side can be calculated as follows:

$$h_i = \frac{Q_h}{A_i(T_m - T_s)} \quad \dots(2)$$

where: $A_i = \pi d_i l$, $T_m = \frac{T_{hi} + T_{ho}}{2}$ and $T_s = \frac{T_1 + \dots + T_6}{6}$

Overall heat transfer coefficient can be calculated as:

$$U_i = \frac{Q_h}{A_i LMTD} \quad \dots(3)$$

where:

$$LMTD = \frac{\Delta T_2 - \Delta T_1}{\ln\left(\frac{\Delta T_2}{\Delta T_1}\right)}, \Delta T_1 = T_{hi} - T_{co}, \Delta T_2 = T_{ho} - T_{ci} \quad \dots(4)$$

The thermal resistance $\frac{\ln(\frac{d_o}{d_i})}{2 \pi k_t l}$ can be neglected ,annuli heat transfer coefficient can be written as:

$$h_o = \frac{1}{\frac{1}{U_o} - \frac{(A_u + \xi_t A_f)}{h_i A_i}} \quad \dots(5)$$

where:

$$A_u = (\pi d_o l - N_f l \delta), \quad A_f = (2 H_f + \delta) N_f l \text{ and } \xi_t = 1 - \frac{A_f}{A_t} (1 - \xi_f) \quad \dots(6)$$

and:

$$U_o = \frac{U_i A_i}{(A_u + \xi_t A_f)} \quad \dots(7)$$

Then Nusselt's number for annuli side can be calculates as:

$$Nu_c = \frac{h_o D_e}{k_c} \quad \dots(8)$$

where:

$$D_e = \frac{4 A_c}{P_h} \quad \dots(9)$$

$$A_c = \frac{\pi}{4} (D_i^2 - d_o^2) - (\delta H_f N_f), \quad P_h = \pi d_o l + 2 H_f N_f^{[10]} \quad \dots(10)$$

In this study, the Reynold's number is calculated by the relation:

$$Re = \frac{\rho V D_{hu}}{\mu} \quad \dots(11)$$

where:

$$D_{hu} = d_i \text{ (laminar flow in the inner tube)} \quad \dots(12-a)$$

$$D_{hu} = D_i - d_o \text{ (turbulent flow in smooth annuli)} \quad \dots(12-b)$$

$$D_{hu} = \frac{4 A_c}{P_w}, \quad P_w = \pi (D_i + d_o) + 2 H_f N_f \text{ (turbulent flow in finned annuli)} \quad \dots(12-c)$$

The effectiveness is the ratio of the actual heat transfer to the maximum possible amount of heat transfer during the operation of heat exchanger. It can be written as follows:

$$\varepsilon = \frac{Q_{act}}{Q_{max}} \quad \text{---(13)}$$

The number of heat transfer units can be defined as:

$$NTU = \frac{U A}{C_{min}} \quad \text{-----(14)}$$

3. Numerical Simulation

ANSYS FLUENT 14 package has been conducted for performing numerical simulation across the heat exchanger using three-dimensional model. The solution of conservation continuity, momentum and energy equations are used to analyze the flow field inside the heat exchanger^[11]. A comparison of heat transfer for (smooth, U-longitudinal) finned tube heat exchanger is carried out. A SOLID WORK PREMIUM 2012 is used to draw the geometries of this work which consist U-longitudinal finned tube heat exchanger with inlet and outlet portions, the outside flow is confined by insulating tube having inlet and outlet portions as shown in **Figure (1)**.

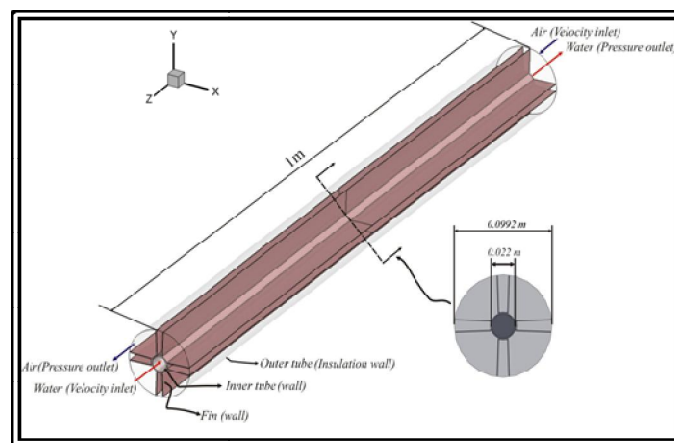


Fig .(1) U- longitudinal finned tube heat exchanger.

3.1 Governing Equations

The governing equations for continuity, momentum, and energy are used to analyze the flow field inside the heat exchanger. The assumptions consist Steady state, Newtonian fluid, incompressible, three dimensional, laminar flow in water side (inner), turbulent flow in air side (annuli), buoyancy effect is assumed to be negligible and radiation heat transfer is not considered. The governing equations are described in the following equations:

For laminar flow:

Continuity equation:

$$\frac{\partial u}{\partial x} + \frac{\partial v}{\partial y} + \frac{\partial w}{\partial z} = 0 \quad \dots(15)$$

Momentum equation:

$$\rho \left(u \frac{\partial u}{\partial x} + v \frac{\partial u}{\partial y} + w \frac{\partial u}{\partial z} \right) = - \frac{dP}{dx} + \mu \left(\frac{\partial^2 u}{\partial x^2} + \frac{\partial^2 u}{\partial y^2} + \frac{\partial^2 u}{\partial z^2} \right) \quad \dots(16.a)$$

$$\rho \left(u \frac{\partial v}{\partial x} + v \frac{\partial v}{\partial y} + w \frac{\partial v}{\partial z} \right) = - \frac{dP}{dy} + \mu \left(\frac{\partial^2 v}{\partial x^2} + \frac{\partial^2 v}{\partial y^2} + \frac{\partial^2 v}{\partial z^2} \right) \quad \dots(16.b)$$

$$\rho \left(u \frac{\partial w}{\partial x} + v \frac{\partial w}{\partial y} + w \frac{\partial w}{\partial z} \right) = - \frac{dP}{dz} + \mu \left(\frac{\partial^2 w}{\partial x^2} + \frac{\partial^2 w}{\partial y^2} + \frac{\partial^2 w}{\partial z^2} \right) \quad \dots(16.c)$$

Energy equation:

$$\rho C_p \left(u \frac{\partial T}{\partial x} + v \frac{\partial T}{\partial y} + w \frac{\partial T}{\partial z} \right) = k \left(\frac{\partial^2 T}{\partial x^2} + \frac{\partial^2 T}{\partial y^2} + \frac{\partial^2 T}{\partial z^2} \right) \quad \dots(17)$$

For turbulent flow:

Continuity equation:

$$\frac{\partial \bar{u}}{\partial x} + \frac{\partial \bar{v}}{\partial y} + \frac{\partial \bar{w}}{\partial z} = 0 \quad \dots(18)$$

Momentum equation:

$$\left(\bar{u} \frac{\partial \bar{u}}{\partial x} + \bar{v} \frac{\partial \bar{u}}{\partial y} + \bar{w} \frac{\partial \bar{u}}{\partial z} \right) + \left(\frac{\partial}{\partial x} (\overline{u'^2}) + \frac{\partial}{\partial y} (\overline{u'v'}) + \frac{\partial}{\partial z} (\overline{u'w'}) \right) = - \frac{1}{\rho} \frac{\partial P}{\partial x} + \nu \nabla^2 \bar{u} \quad \dots(19)$$

$$\left(\bar{u} \frac{\partial \bar{v}}{\partial x} + \bar{v} \frac{\partial \bar{v}}{\partial y} + \bar{w} \frac{\partial \bar{v}}{\partial z} \right) + \left(\frac{\partial}{\partial x} (\overline{u'v'}) + \frac{\partial}{\partial y} (\overline{v'^2}) + \frac{\partial}{\partial z} (\overline{v'w'}) \right) = - \frac{1}{\rho} \frac{\partial P}{\partial y} + \nu \nabla^2 \bar{v} \quad \dots(20)$$

$$\left(\bar{u} \frac{\partial \bar{w}}{\partial x} + \bar{v} \frac{\partial \bar{w}}{\partial y} + \bar{w} \frac{\partial \bar{w}}{\partial z} \right) + \left(\frac{\partial}{\partial x} (\overline{u'w'}) + \frac{\partial}{\partial y} (\overline{v'w'}) + \frac{\partial}{\partial z} (\overline{w'^2}) \right) = - \frac{1}{\rho} \frac{\partial P}{\partial z} + \nu \nabla^2 \bar{w} \quad \dots(21)$$

Energy equation:

$$\bar{u} \frac{\partial \bar{T}}{\partial x} + \bar{v} \frac{\partial \bar{T}}{\partial y} + \bar{w} \frac{\partial \bar{T}}{\partial z} = \alpha \nabla^2 \bar{T} + \left(-\frac{\partial}{\partial x} (\overline{u'T'}) - \frac{\partial}{\partial y} (\overline{v'T'}) - \frac{\partial}{\partial z} (\overline{w'T'}) \right) \quad \dots(22)$$

Boussinesq Assumption:

$$G_{\mathcal{K}} = \mu_t S^2 \quad \dots(23)$$

where:

S = the modulus of the main rate-of-strain tensor.

$G_{\mathcal{K}}$ = generation of turbulent kinetic energy due to mean velocity gradients.

\mathcal{K} equation:

$$\rho \left(\bar{u} \frac{\partial \mathcal{K}}{\partial x} + \bar{v} \frac{\partial \mathcal{K}}{\partial y} + \bar{w} \frac{\partial \mathcal{K}}{\partial z} \right) = \left[\left(\mu + \frac{\mu_t}{\sigma_{\mathcal{K}}} \right) \left(\frac{\partial^2 \mathcal{K}}{\partial x^2} + \frac{\partial^2 \mathcal{K}}{\partial y^2} + \frac{\partial^2 \mathcal{K}}{\partial z^2} \right) \right] + G_{\mathcal{K}} - \rho \epsilon \quad \dots(24)$$

ϵ equation:

$$\rho \left(\bar{u} \frac{\partial \epsilon}{\partial x} + \bar{v} \frac{\partial \epsilon}{\partial y} + \bar{w} \frac{\partial \epsilon}{\partial z} \right) = \left[\left(\mu + \frac{\mu_t}{\sigma_{\epsilon}} \right) \left(\frac{\partial^2 \epsilon}{\partial x^2} + \frac{\partial^2 \epsilon}{\partial y^2} + \frac{\partial^2 \epsilon}{\partial z^2} \right) \right] + C_{1\epsilon} \frac{\epsilon}{\mathcal{K}} G_{\mathcal{K}} - C_{2\epsilon} \rho \frac{\epsilon^2}{\mathcal{K}} \quad \dots(25)$$

3.2 Implementation of Boundary Conditions

To estimate the performance of the present heat exchanger, some introductory requirements of the physical model are defined adequately as follows:

- **Inlet Boundary Conditions:**

Reynolds number was specified 270-1900 for inner diameter . On the other hand the temperature inlet of the inner tube is (60) °C and in annuli (20) °C.

- **Pressure Outlet Boundary Conditions:**

The outlet domain is specified as pressure outlet for both sides.

- **Wall Boundary Condition:**

No slip boundary condition is specified in the wall of the inner tube. These conditions are used to bound fluid and solid region.

3.3 Mesh Generation

Unstructured solver is used in FLUENT software for unstructured mesh. In unstructured mesh, the pattern of connections varies from point to point and the connectivity of the mesh must be explicitly described by an appropriate data structure. The model is meshed with GAMBIT software. The refinement and generation of mesh system are very crucial to predict the heat transfer in sophisticated geometries, thus the density and distribution of the mesh lines play distinct roles for accuracy^[12]. During this study, many number of cells has been taken and an average of (11) million cells is found as the optimum number regarding with the best numerical prediction of present model.

In this study triangular element type is employed for surface mesh and tetrahedron element type is used for three dimensional geometry since it has priority in the sophisticated geometries.

Figures (2) and (3) show the mesh of present model and mesh topology respectively.

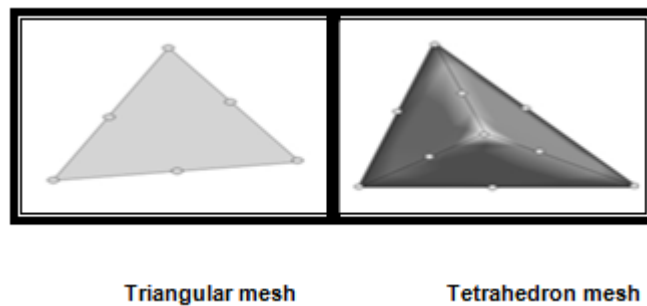


Fig .(2) Mesh topology.

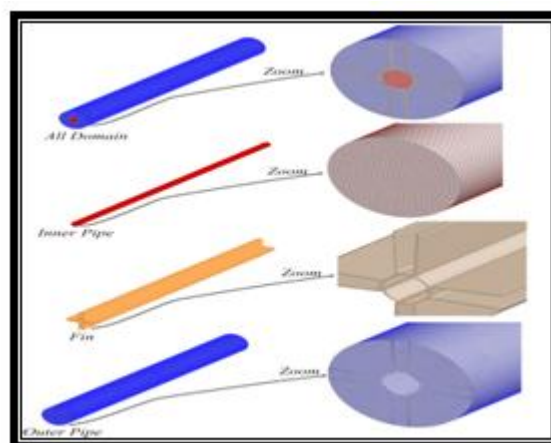


Fig .(3) Mesh of the physical model and fluid domain.

3.4 Convergence Criterion

For the present study, the scaled residual for continuity, velocities and energy equations are monitored during the iterative solutions and the values are taken into consideration for the convergence as follow:

Residual of continuity = 0.003

Residual for velocities = 0.003

Residual for energy = 10^{-6}

$\mathcal{K} = 10^{-3}$, $\epsilon = 10^{-3}$

Number of iterations = 4000

Figure (4) shows scaled residual history for governing equations of present study.

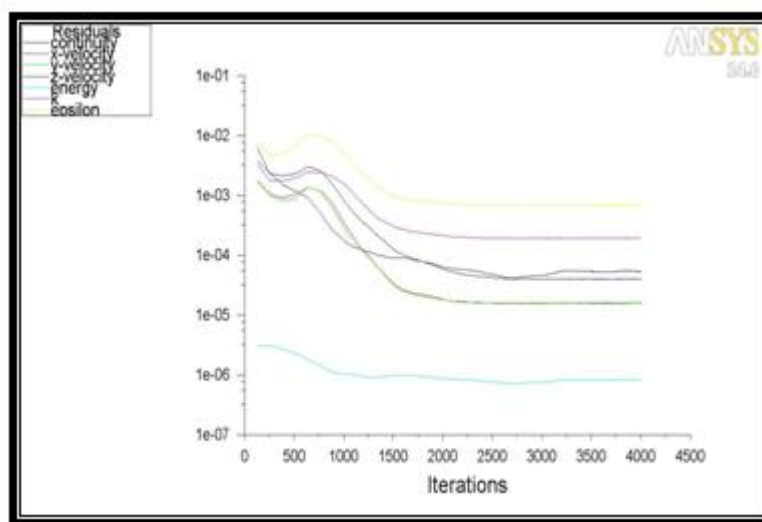


Fig .(4) Residual history for governing equations of present study.

4. Experimental Test Rig

Figures (5) and (6) show the photograph of test rig and schematic diagram of test section. Test rig consists test section, air and water supply system, measuring devices and supplements. Various kinds of measuring devices have been used such as digital anemometer, temperature recorder, water flow meter, thermocouples and temperature probes. The test section contains two parts, the first consists insulated tube has been manufactured from galvanized material of (150mm) inner diameter, (1.56m) length and (1mm) thickness. It is insulated from inside by sheet and roll insulation (arm flux) and from outside by glass wool. These insulations have been used to reduce the heat losses to the surrounding. The second part is an internal copper tube without or with U–longitudinal copper fins. The smooth copper tube has (1m) long and (0.022m,0.0239m) inner and outer diameter respectively. Pairs of U-shaped fins are manufactured from copper, they are welded to the external surface of tube by silver welding technique to form U–shaped channels having (1m) length, (0.038m) height,

(1mm) thickness and (8.2mm) distance between every pair and (9mm) pitch between each two pairs of fins. A water pump is used for pumping the water in pipes through the water cycle and test section. It has (30liter/minute) volumetric flow rate and centrifugal blower is employed to provide air for the test section through diffuser and fully developed pipe.



Fig .(5) Photograph of test rig.

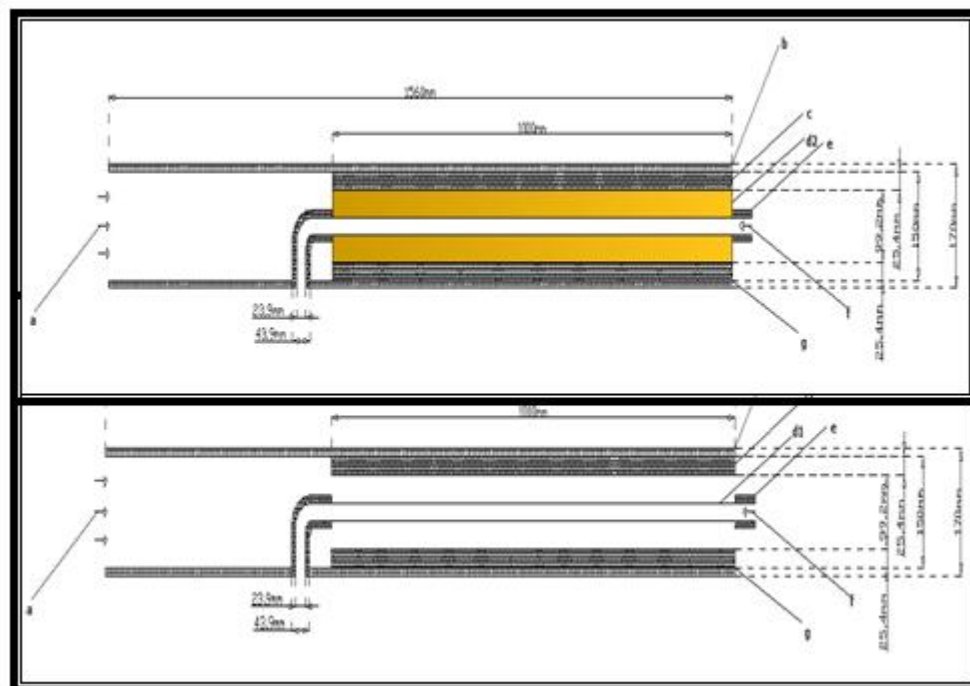


Fig .(6) Geometry of present test sections: a. cold air. b. outer insulation(glass wool)for air side. c. inner insulation (arm flux) for air side. d1. smooth tube .d2. finned tube. e. insulation (arm flux) for water side. f. hot water.

5. Results and Discussions

The performance of the present heat exchanger has been discussed through the following paragraphs. **Figure (7)** explain the variation of annuli heat transfer coefficient with the air mass flow rate for smooth and U–longitudinal finned tube. Air heat transfer coefficient increased due to turbulence introduced by increasing air velocity. Heat transfer coefficient for finned tube is greater than of smooth tube due to increase surface area by fins. During this study the range of enhancement in air heat transfer coefficient was(1.744 to 2.534). **Figures (8)** shows the effect of different water Reynold's number on the inner heat transfer coefficient. It can be seen from these figures that water side heat transfer coefficient increases due to turbulence generated by increasing of water Reynold's number indicating maximum increase of (62.5%). **Figure (9)** show the variation of the air side temperature difference with the air mass flow rate for smooth and U–longitudinal finned tube. The air temperature difference decreases by (44%) as a result of increase air mass flow rate. The air side temperature difference in finned tube is larger by (65%) than that of smooth tube due to enhancement by increasing the surface area. **Figures (10)** illustrates the variation of the water side temperature difference with the water Reynold's number for smooth and U–longitudinal finned tube. The water side temperature difference tends to decrease (67%) by increasing water Reynold's number. **Figures (11) and (12)** illustrate the variation of effectiveness with number of transfer units in present study. Positive relationship can be noted in these figures due to the dependence of the number of transfer units and effectiveness on the overall heat transfer coefficient. Effectiveness of finned tube is greater than that of smooth tube by (68%). Overall heat transfer coefficient represents the overall ability of conductive and convective resistant's to heat transfer and it is commonly applied to observe the behavior in the heat exchanger. **Figure (13)** illustrate the relation between overall heat transfer coefficient based on air side and heat dissipation calculating from the water side. It can be seen that overall heat transfer coefficient increased by increasing heat dissipation by (38%). **Figure (14)** show the variation of inner tube surface temperature with axial distance ratio at various air Reynold's number. It can be noted from these figures that surface temperature decreases with axial distance ratio due to the counter flow arrangement of the present heat exchanger. Surface temperature increase with increase water Reynold's number by (30%). Experimental results of test rig are validated in this study by numerical simulation produced by ANSYS FLUENT 14 as shown in **Figure (15)**. In this figure, the surface temperature of inner tube has been illustrated with axial distance ratio. Good agreement is observed with 9% difference between experimental and numerical results. **Figures (16)** show the temperature and velocity contours of smooth tube heat exchanger at various axial distances. It can be noted from these figures that the maximum air and water temperatures appears at $Z/d = 0$ and the minimum temperatures appears at $Z/d = 45$. Velocity contours in this figure show that air inlet velocity distribution at $Z/d = 45$ is uniform and tends to decrease inside heat exchanger near the walls of inner and outer tubes as shown at Z/d from 36 to 0. **Figure (17)** shows the water velocity in

axial distance. Water velocity at the center increases while the velocity gradient near the wall decreases with increasing axial distance as shown at $Z/d = 9, 27$, and 45 . **Figures (18)** reveals the temperature and velocity contours of U-longitudinal finned tube heat exchanger at various axial distances ratio. Results showed significant heat transfer augmentation in heat exchanger at Z/d from 0 to 45 for air and water sides. The effect of adopting fins on heat transfer enhancement is apparent in both sides. Velocity contours in this figure reveal that air velocity is uniform at $Z/d = 45$ while it increases at the center between every two pairs of fins and U channels at Z/d from 36 to 0. The effect of wall on decreasing the velocity in air and water sides is apparent in **Figure (19)** Empirical correlations of Nusselt's number were estimated from the experimental results by using DGA program and according to algebraic expression of the form $(Y = a X_1^{N_1} X_2^{N_2} \dots)$ for present heat exchanger as follows:

$$Nu_c = 0.909 Re^{0.433} Pr^{1/3}$$

Above relation are valid for $8000 \leq Re_c \leq 18000$

$$Nu_h = 0.112 (Re Pr)^{0.562}$$

Above relation are valid for $270 \leq Re_h \leq 1900$. **Figures (20) to (21)** show the comparison between experimental and predicted number for air and water sides.

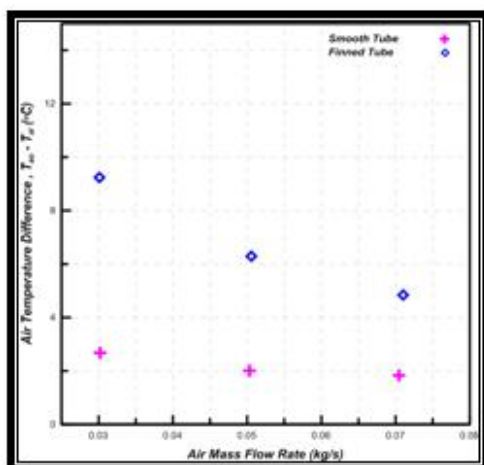


Fig .(7) Effect of air mass flow rate on air heat transfer coefficient.

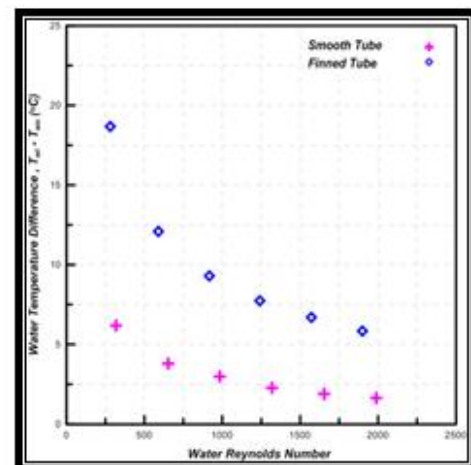


Fig .(8) Effect of water Reynold's number on water heat transfer coefficient.

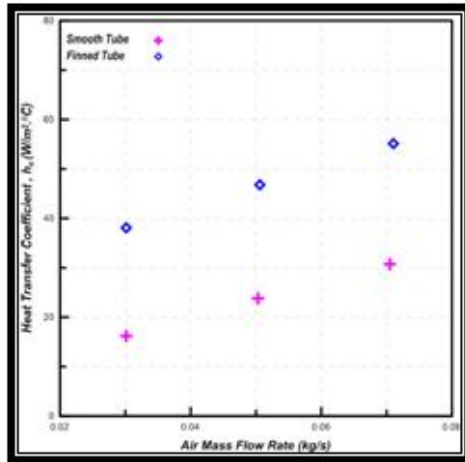


Fig .(9) Effect of air mass flow rate on air temperature difference.

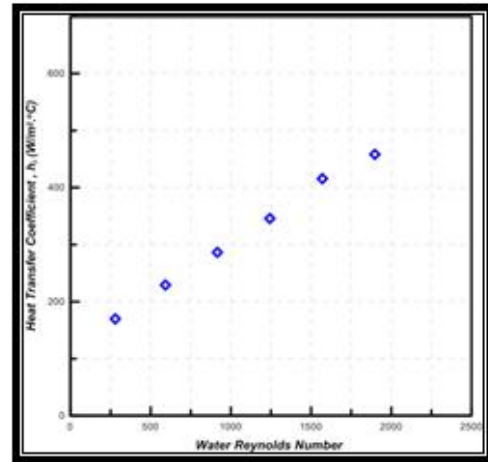


Fig .(10) Effect of water Reynold's number on water temperature difference.

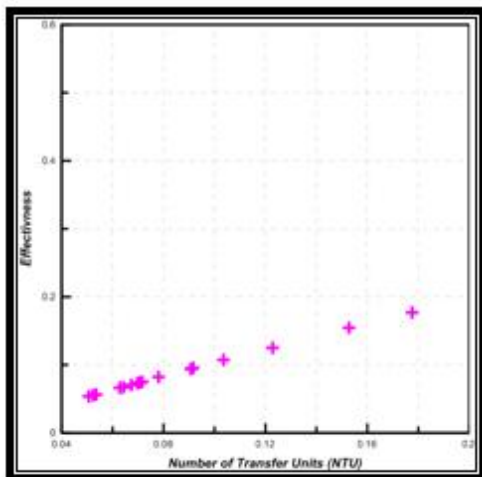


Fig .(11) Variation of effectiveness with number of transfer units in smooth tube.

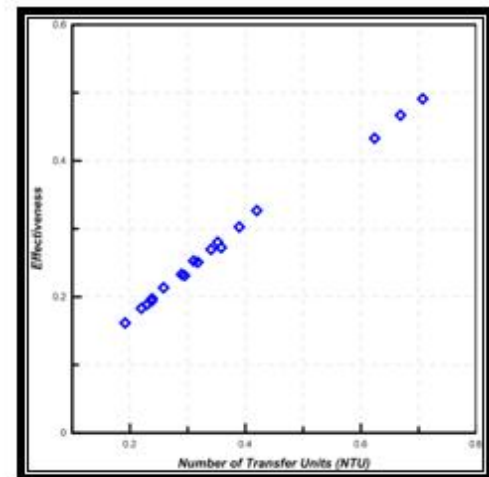


Fig .(12) Variation of effectiveness with number of transfer units in finned tube.

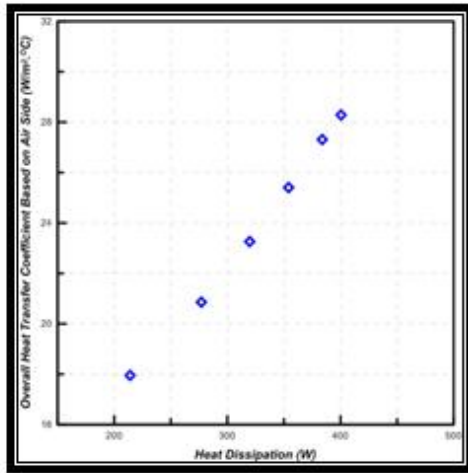


Fig .(13) Effect of heat dissipation on U_o .

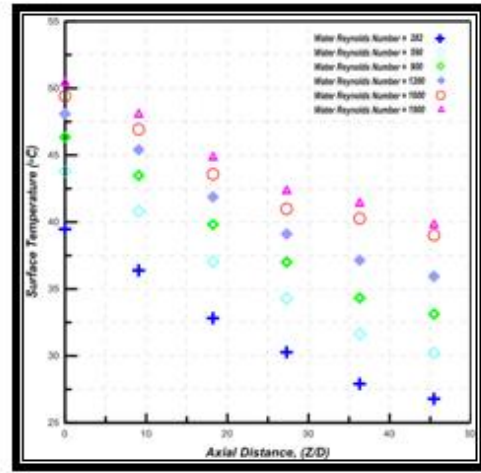


Fig .(14) Variation of surface temperature with axial distance ratio.

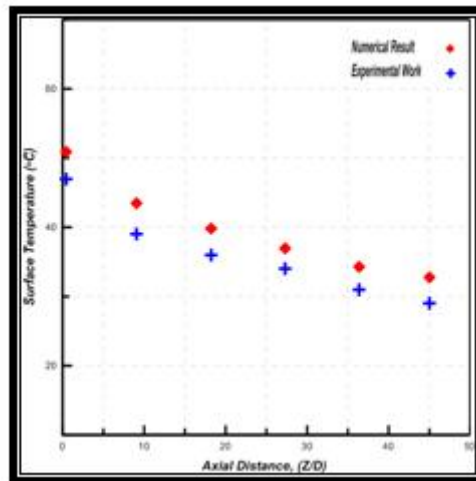


Fig .(15) Validation of experimental work by numerical simulation.

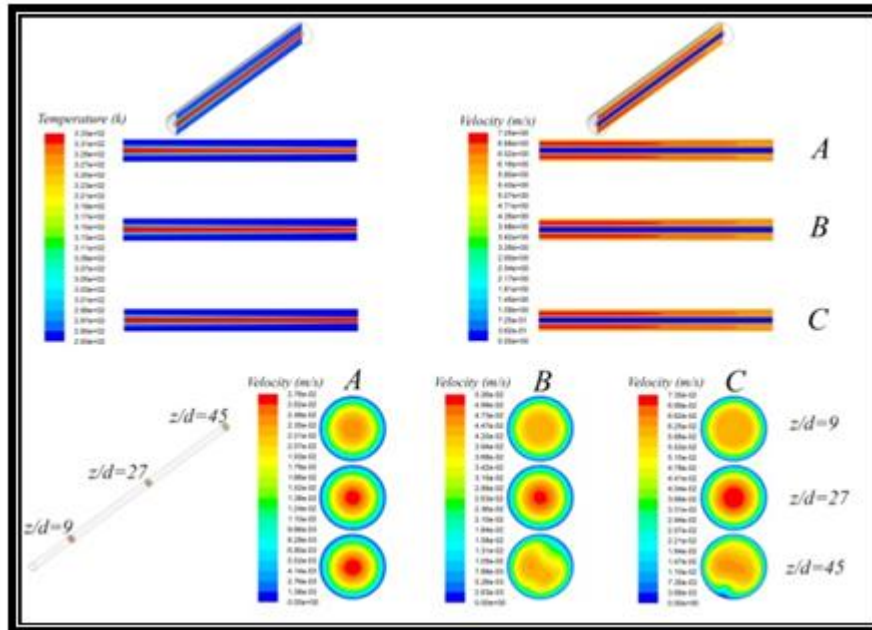


Fig .(16) Temperature and velocity contours of smooth tube heat exchanger.

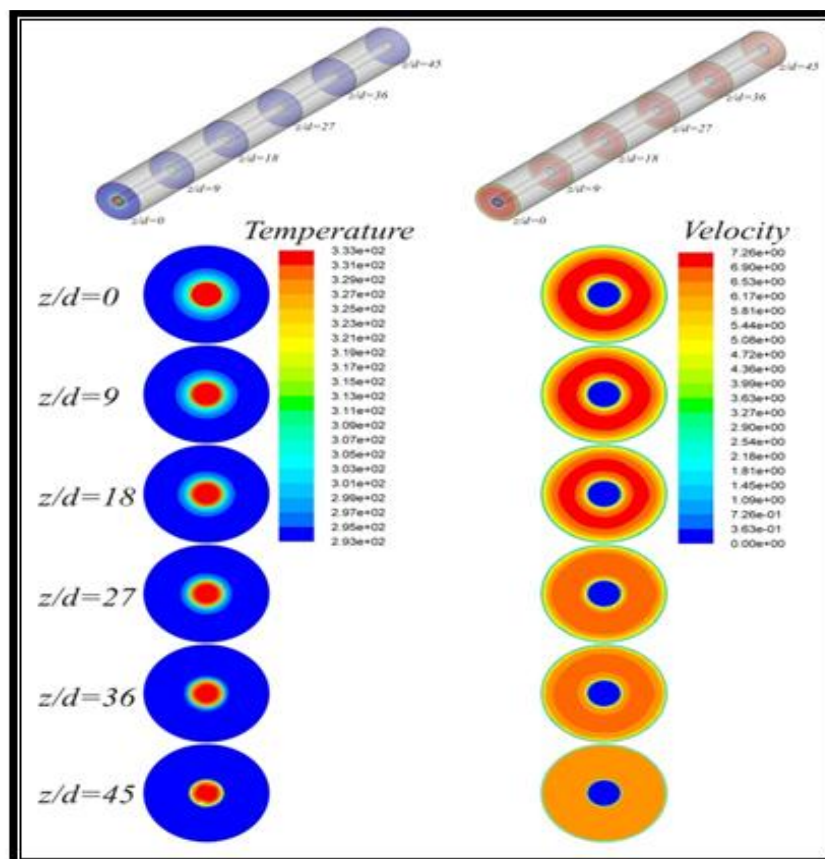


Fig .(17) Temperature and velocity contours along (x-axis) at $\dot{m}_c = 0.05$ kg/sec and (A. $Re_h = 590$. B. $Re_h = 1200$. C. $Re_h = 1900$). for U-longitudinal finned tube heat exchanger.

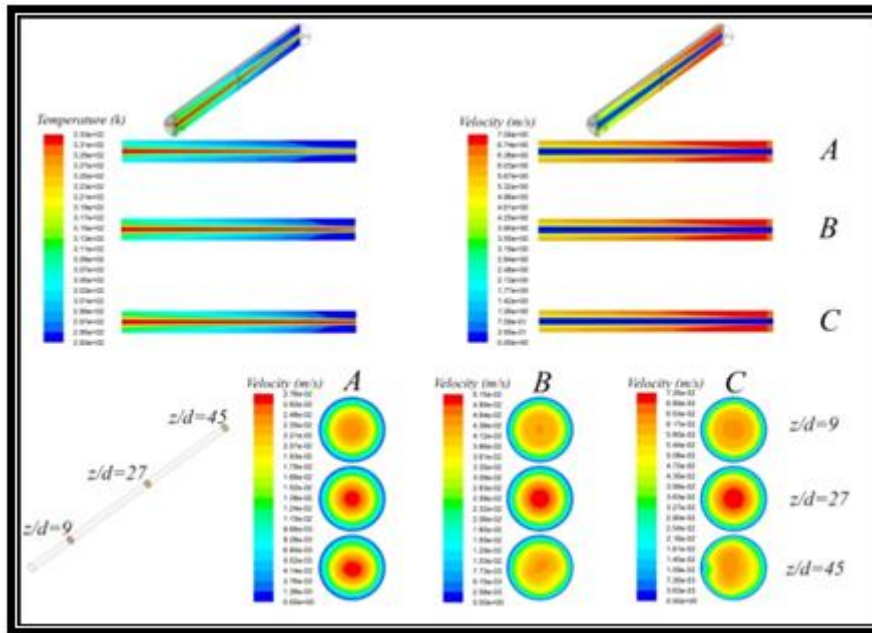


Fig .(18) Temperature and velocity contours of U-longitudinal finned tube heat exchanger.

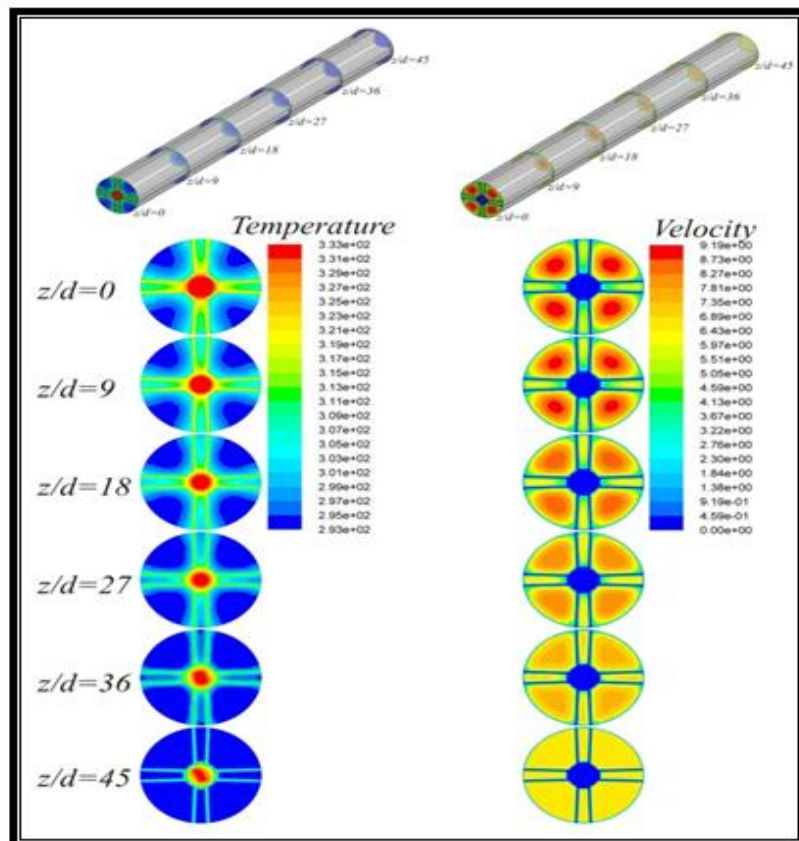


Fig .(19) Temperature and velocity contours along (x-axis) at $\dot{m}_c = 0.05$ kg/sec and (A. $Re_h = 590$. B. $Re_h = 1200$. C. $Re_h = 1900$). for U-longitudinal finned tube heat exchanger.

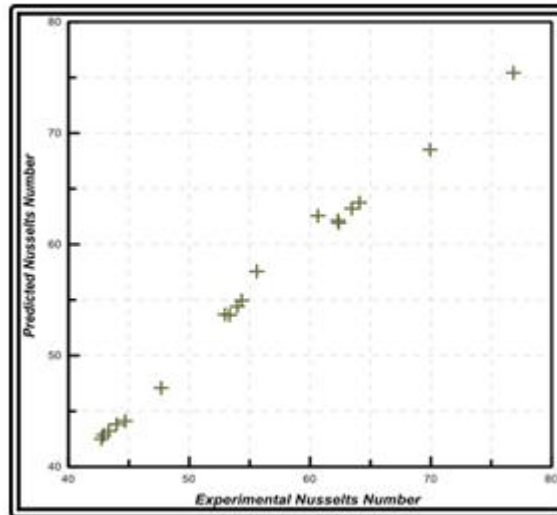


Fig .(20) Comparison between predicted and experimental Nusselt's number for air side.

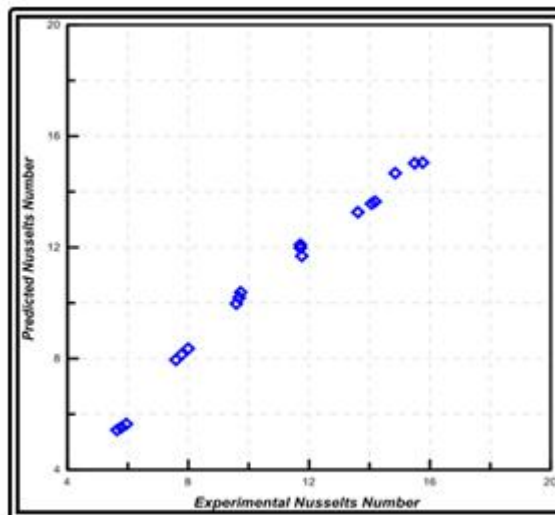


Fig .(21) Comparison between predicted and experimental Nusselt's number for water side.

6. Conclusions

The conclusions resulting from present study will be outlined in the following points:

1. The heat transfer augmentation is apparent when adopting fins on outer surface of inner tube in present heat exchanger. This enhancement appears clearly in heat dissipation and air heat transfer coefficient indicating (2.79 to 3.43) and (1.744 to 2.534) times than that of smooth tube respectively .

2. Air side temperature difference is directly proportional with the water Reynold's number and decreased by (44%) with increasing the air mass flow rate.
3. Water side temperature difference is directly proportional to the air mass flow rate and decreased by (67%) with increasing the water Reynold's number .
4. Results of numerical simulation showed that adding fins would enhance heat dissipation through heat exchanger. It is noted that heat transfer behavior increases within present model as air mass flow rates and water Reynold's numbers increases .
5. Numerical simulation by FLUENT package is successful for predicting heat transfer and fluid flow in the present heat exchanger.

References

1. Arthur E. Bergles, "The Imperative to Enhance Heat Transfer", Heat Transfer Enhancement of Heat Exchangers, pp.(13–29), 1999.
Taborek Jerry, "Double-Pipe and Multitube Heat Exchangers with Plain and Longitudinal Finned Tubes", Heat Transfer Eng., Vol.18 (2) : pp. (34–45), 1997.
2. G. Fabbri, "Optimum Performances of Longitudinal Convective Fins with Symmetrical and Asymmetrical Profiles", International Journal of Heat and Fluid Flow, Vol.20, pp.643-641, 1999.
3. Yu B., Tao W. Q., "Pressure Drop and Heat Transfer Characteristics of Turbulent Flow in Annular Tubes with Internal Wave-Like Longitudinal Fins", Heat and Mass Transfer, Vol.40, pp.(643–651), 2004.
4. Mir N. A., Syed K. S. and Mazhar Iqbal, "Numerical Solution of Fluid Flow and Heat Transfer in the Finned Double Pipe", Journal of Research, Bahauddin Zakariya University, Multan, Pakistan, Vol.15, No.3, pp.(253-262), 2004.
5. Syed K. S., Mazhar Iqbal, Mir N. A., "Convective Heat Transfer in the Thermal Region of Finned Double-pipe", Heat Mass Transfer, Vol.43, pp. (449–457), 2007.
6. Iqbal Z., Syed K. S., Ishaq M., "Optimal Fin Shape in Finned Double Pipe with Fully Developed Laminar Flow", Applied Thermal Engineering , pp. (1202-1223), 2013.
7. Frank P. Incropera, David P. Dewitt, Theodore L. Bergman, Adrienne's S. Lavine, "Introduction to Heat Transfer", John Wiley & Sons Inc. 2007.
8. Ramesh K. Shah and Dušan P. Sekulic, "Fundamentals of Heat Exchanger Design ", Jon Wiley & Sons, 2003.
9. Sahiti N., Durst F., Dewan A., "Heat Transfer Enhancement by Pin Elements", International Journal of Heat and Mass Transfer, Vol.48, pp. (4738–4747), 2005.
10. "Ansys Fluent User's Guide", Ansys, Inc, Southpointe 275 Technology Drive Canonsburg, PA15317, 2011.
11. Rebay S. , "Efficient Unstructured Mesh Generation By Means of Delainay Triangulation and Bowyer-Watson Algorithm", Journal of Computational Physics, pp.(125-138), 1993.
- 12.